# Targeted IS-element sequencing uncovers transposition dynamics during selective pressure in enterococci

Joshua M. Kirsch[1], Shannon Ely[1], Madison E. Stellfox[2], Karthik Hullahalli[3], Phat Luong[1], Kelli L. Palmer[3], Daria Van Tyne[2], Breck A. Duerkop[1*]

[1]Department of Immunology and Microbiology, University of Colorado School of Medicine, Aurora, CO 80045, USA

[2]Department of Medicine, Division of Infectious Diseases, University of Pittsburgh, Pittsburgh, PA 15214, USA

[3]Department of Biological Sciences, University of Texas at Dallas, Richardson, TX 75080, USA

*Correspondence: Breck A. Duerkop breck.duerkop@cuanschutz.edu

**Abstract**

Insertion sequences (IS) are simple transposons implicated in the genome evolution of diverse pathogenic bacterial species. Enterococci have emerged as important human intestinal pathogens with newly adapted virulence potential and antibiotic resistance. These genetic features arose in tandem with large-scale genome evolution mediated by mobile elements. Pathoadaptation in enterococci is thought to be mediated in part by the IS element IS256 through gene inactivation and recombination events. However, the regulation of IS256 and the mechanisms controlling its activation are not well understood. Here, we adapt an IS256-specfic deep sequencing method to describe how chronic lytic phage infection drives a widespread expansion of IS256 in *E. faecalis* and how antibiotic exposure is associated with IS256 expansion in both *E. faecalis* and *E. faecium* during a clinical human infection. We show through comparative genomics that IS256 is primarily found in hospital-adapted enterococcal isolates. IS256 transposase gene expression analyses reveal that IS256 mobility is regulated at the transcriptional and translational levels in *E. faecalis*, indicating tight control of IS256 activation in the absence of selective pressure. Our findings reveal that stressors such as phages and antibiotic exposure drives rapid genome-scale transposition in the enterococci. IS256 expansion can therefore explain how selective pressures mediate evolution of the enterococcal genome, ultimately leading to the emergence of dominant nosocomial lineages that threaten human health.

## Introduction

Enterococci, including the human commensals *Enterococcus faecalis* and *Enterococcus faecium*, are opportunistic pathogens of public health concern due to their acquisition of antibiotic resistance and virulence traits[1]. Enterococcal infections are a leading cause of infective endocarditis[2, 3] and 30% of nosocomial infections are vancomycin resistant[4, 5]. Antibiotic resistance in enterococci is often encoded on mobile genetic elements, including plasmids and composite transposons[6]. Plasmids, especially those containing Inc18, Rep_3, and RepA-N replicon-containing plasmids, frequently encode resistance genes to diverse antibiotics, including chloramphenicol, erythromycin, and gentamicin[7, 8]. Composite transposons are typically organized with a cargo gene (such as an antibiotic resistance gene) flanked by insertion sequence (IS) elements. Examples in the enterococci include Tn4001 or Tn4031, which carries gentamicin resistance genes[9] and Tn1546 and Tn1547, which carry the vancomycin resistance *vanA* and *vanB* operons, respectively[10, 11].

To combat clinically relevant enterococcal strains, new therapeutics are urgently needed. Recently, the concept of using bacterial viruses (bacteriophages or phages) to treat multi-drug resistant (MDR) bacteria is being revisited[12]. Phage therapy case studies show that these viruses can be efficacious against refractory MDR bacteria in human patients[13, 14, 15, 16, 17]. However, bacterial resistance to phage infection develops quickly[18, 19, 20, 21] and the lessons learned from the past century of antibiotic use suggest that bacteria will gain resistance to phage infection after widespread phage treatment[22]. Acquired phage resistance, although beneficial to bacteria in the face of phage pressure, can come with fitness costs that dampen antibiotic resistance and virulence[12, 23, 24, 25]. Therefore, it is imperative to fully understand the mechanisms that promote phage-resistance in bacteria, and the phenotypic outcomes of phage resistance. With this knowledge it will be possible to use phage resistance as a tool that can be leveraged against bacteria to enhance current antibacterial therapeutics.

Enterococci have remarkably diverse genomes containing numerous mobile elements that contribute to their adaptation and evolution[26, 27, 28]. These include plasmids, prophages, and transposable insertion sequence (IS) elements. Pathogenic enterococci frequently contain multiple IS elements, and IS elements appear to be a feature of newly-adapted nosocomial strains[29]. In the widely studied nosocomial type-strain *E. faecalis* V583, there are 38 IS elements consisting of 11 different types[26]. IS256 is the most abundant IS element in the *E. faecalis* V583 genome, with six chromosomal copies and four plasmid copies. IS256 is also common in other gram-positive bacteria, including staphylococci, where it has been widely studied[30, 31, 32]. In the staphylococci, IS256 mediates clinically-relevant phenotypes, such as small colony variation[33], biofilm formation[31], and antibiotic resistance[34]. The transcription factor σ-B negatively regulates IS256 transposition in the staphylococci through the production of a 3' antisense RNA[31, 35]. IS256 is a crucial component for enterococcal genome adaptation. In *E. faecalis* V583, the virulence factor cytolysin is attenuated by IS256 and related IS905 insertions[36]. Additionally, copies of IS256 in the *E. faecalis* V583 pheromone-responsive plasmids pTEF1 and pTEF2 recombine with chromosomal IS256 copies to mobilize broad regions of the *E. faecalis* genome[37]. A related IS element, IS16, has been shown to be highly abundant in hospital-adapted *E. faecium* isolates, suggesting that IS16 may aid in the success of *E. faecium* as a nosocomial pathogen[38]. Considering IS elements are likely involved in the pathoadaptation of the enterococci, little is known about how these elements are regulated and what events lead to their activation.

In this work, we investigated both the regulation and spread of IS256 transposition in *E. faecalis* and *E. faecium*. We found that IS256 is present in multiple, genetically disparate isolates of both species, and is enriched in hospital adapted lineages. At steady state, IS256 produces a wealth of low abundance insertions throughout the chromosome and is regulated at both the transcriptional and translational levels to tightly control activation. We discovered that phage infection and antibiotic usage in different biological settings were associated with a

dramatic expansion of IS256 insertion events. In the case of phage infection, cell populations experiencing IS256 expansion maintained phage genomes as independently replicating episomes and a subpopulation of these cells chronically shed phage particles throughout growth. Phage shedding provided a competitive advantage during co-culture with phage-susceptible enterococci, but this advantage is lost when co-cultured with phage-resistant enterococci. This suggests that phage genome carriage is a strong selective pressure that drives IS256 mobilization and can be used to occupy an environmental niche when competing with phage-susceptible bacterial strains. Lastly, we investigated how IS256 diversifies enterococcal genomes in a chronically infected patient, and found that IS256 insertion abundances in vivo coincided with specific antibiotic usage. Together, this work sheds light on how IS elements are regulated and expanded in enterococcal genomes during both phage predation and clinical infection, and provides evidence for phage carriage as an important selective pressure that promotes IS256 mobility. Furthermore, this work suggests that therapeutic use of both phages and antibiotics could cause rapid and widespread enterococcal genome evolution for which the physiological consequences are unknown.

## Results

### *IS256 is common within enterococcal lineages associated with hospital adaptation and pathogenesis*

IS256 is an important factor driving the pathoadaptation of *E. faecalis*[36], yet it is unknown how widely IS256 is distributed among *E. faecalis* strains. To answer this, we searched all available *E. faecalis* genomes from NCBI RefSeq (2065 genomes) for IS256 transposases with 100% amino acid similarity to the IS256 transposase copies found in *E. faecalis* V583. A total of 232 genomes contained one or more IS256 sequences (Fig. 1A). The sporadic distribution of IS256 within the *E. faecalis* phylogenetic tree suggests that IS256 is a recent addition to many *E. faecalis* genomes and has arisen within multiple discrete lineages of this species. To further

characterize the distribution of IS256 across *E. faecalis* strains, we performed in silico multilocus sequence typing (MLST) on all *E. faecalis* genomes and compared the proportions of genomes with and without IS256 in each sequence type (ST) (Fig. 1B). IS256 occurs within a variety of ST clades and is most abundant in in ST6, ST103, ST778, and ST388 genomes, all of which are associated with hospital-adapted, opportunistic pathogenic lineages (Table S1A)[39, 40, 41, 42]. We compared the abundances of different virulence factors between genomes with and without IS256 (Fig. 1C & Table S1C). IS256-containing genomes are enriched for multiple virulence factors compared to genomes lacking IS256, demonstrating that IS256 preferentially occurs in hospital-acquired and virulent *E. faecalis* strains. We next expanded this analysis to include all *E. faecium* genomes from RefSeq (2306 genomes) and similar to *E. faecalis*, *E. faecium* IS256 is primarily found in the nosocomial lineages ST17, ST664, ST736, and ST18 (Fig. 1D-E and Table S1B)[43, 44]. Although *E. faecium* IS256-containing genomes have a significant enrichment in some virulence factors, this was less than *E. faecalis* (Fig. 1F and Table S1D). Finally, IS256 is more frequently found in *E. faecium* genomes compared to *E. faecalis* genomes, confirming prior research (Fig. 1G)[45]. Together these data show that IS256 is widely distributed within the enterococci and is preferentially found in nosocomial and virulent isolates.

### *IS-Seq identifies widespread movement of IS256 in E. faecalis that is transcriptionally and translationally controlled*

Previously, IS256 sequences were identified as hot spots in *E. faecalis* V583 that facilitated the integration of the endogenous plasmids pTEF1 and pTEF2, leading to the mobilization of the pathogenicity island and other chromosomal regions[37]. Instances of IS256 insertions leading to the inactivation of *E. faecalis* genes involved in diverse phenotypes have been described[19, 46, 47, 48]. However, we lack a complete understanding of IS256 mobility across the *E. faecalis* genome during selective pressures that would potentially drive IS256 activation and genome diversification. To assess genome-wide IS256 insertions in *E. faecalis* we adapted

a next-generation sequencing (NGS) enrichment technique for use with IS256. This technique, IS-Seq, includes IS256 amplicon enrichment during NGS library construction followed by read mapping of IS256-chromosomal junctions to identify specific IS256 insertion locations (Fig. S1)[49]. Similar techniques have been used to identify IS element insertions in *Acinetobacter*[50] and *Mycobacterium*[51]. IS-Seq of wild-type (WT) *E. faecalis* V583 under steady state conditions identified the known IS256 locations in the chromosome and on the three pTEF plasmids (Fig. 2A & S2). One of the IS256 copies on pTEF1 lacks a canonical left inverted repeat (IR), preventing binning of the IS-Seq reads originating from this locus. Numerous low abundance IS256 insertions are observed throughout the *E. faecalis* genome, indicating promiscuous movement of the element within subpopulations of cells (Fig. 2A). The three replicate cultures tested in Fig. 2A show that each *E. faecalis* population analyzed has a unique repertoire of IS256 insertions. We hypothesize that these low abundance steady-state insertion events provide a mechanism for rapid genome diversification following exposure to selective pressures.

To understand how IS256 is regulated in *E. faecalis* under steady state conditions, we investigated possible mechanisms of repression of the IS element. First, we assessed the transcription of the IS256 transposase (Tnp) gene. During growth in rich media, IS256 gene transcription modestly increases during logarithmic growth, and doubles in comparison to the expression of the reference gene *clpX* (Fig. 2B). Considering there are 10 copies of IS256 in *E. faecalis* V583, each IS256 copy achieves 1/5$^{th}$ the transcriptional activity of a single *clpX* gene. Thus, the relatively weak IS256 promoter may limit over-activation of the element. Next, we investigated whether IS256 is translationally regulated. Other IS elements have been reported to be controlled by expression of antisense small RNAs (asRNA)[52]. These asRNAs bind to sense transcripts at or before the start codon and ribosome binding site to prevent translation of the sense transcript. We reanalyzed a publicly available stranded RNA-Seq dataset of *E. faecalis* V583[53] by aligning reads to an IS256 element with delineation of the sense and antisense alignments (Fig. 2C). The translational start site (TSS) of IS256 has not been

181 experimentally confirmed in any bacterial species and is predicted to occur in the 5' terminus of
182 the element[54]. We demonstrate that IS256 has two TSSs indicated by high antisense read
183 mapping coverage, demonstrating that antisense inhibition is present at both TSSs. If translation
184 initiates at the site-2 TSS this would produce a truncated IS256 Tnp. It is unclear whether this
185 truncated IS256 Tnp would function similar to the full-length IS256 Tnp. Upon further
186 investigation of these TSSs and their asRNAs, we found that the site-1 asRNA is likely under
187 the control of a canonical σ-70 promoter. To identify if this asRNA controls IS256 Tnp
188 translation, we constructed an IS256 Tnp-GFP translational reporter. This construct consists of
189 an IS256 Tnp coding sequence fused in frame at its C-terminus to a green fluorescence protein
190 (GFP) gene. GFP fluorescence serves as a proxy for translation of the IS256 Tnp. In addition,
191 we built a version of the IS256 Tnp-GFP fusion lacking the predicted -10 element of the site-1
192 asRNA. We transformed these constructs into *E. faecalis* OG1RF, a strain that lacks native
193 IS256 elements and IS256-derived asRNAs in its genome, and measured GFP fluorescence in
194 these cells (Fig. 2D). In cells lacking the site-1 asRNA, there is significantly higher GFP
195 fluorescence compared to cells with an intact site-1 asRNA promoter, demonstrating that these
196 asRNAs repress IS256 Tnp translation. These results show that in *E. faecalis* IS256 is regulated
197 by multiple mechanisms at both the transcriptional and translational levels.
198
199 ***IS256 selection during phage predation***
200 Our previous work suggested that phage predation increases IS256 transposition in *E.*
201 *faecalis* V583 and is used as a mechanism of phage resistance[18]. To determine if phage
202 selective pressure results in the expansion of IS256 mobility in *E. faecalis*, we challenged *E.*
203 *faecalis* V583 with the phage phi19[18]. Following phage exposure, we isolated single colonies
204 that were resistant to phi19. Whole genome sequencing (WGS) of these phage-resistant
205 isolates predicted an expansion of new IS256 insertions in phi19 resistant isolates (referred to
206 as 19RS strains) (Fig. 3A). Among the new IS256 insertions in 19RS strains, we found that an

insertion was predicted in the 3' end of *epaX*, a glycosyltransferase gene involved in the biosynthesis of the enterococcal polysaccharide antigen that is required for infection by phi19[18]. To verify this insertion and its orientation, we performed PCR using genomic DNA (gDNA) from four 19RS strains and wild type (WT) *E. faecalis* V583 (Fig. 3B). We found that all 19RS strains harbored an IS256 insertion in *epaX* in both the positive and negative strand orientations. This IS256 insertion likely prevents functional EpaX from being expressed blocking phage infection. Recently, Lossouarn et al. identified IS256 insertions inactivating *epaX*, confirming that an IS256 insertion in *epaX* is sufficient to prevent phage infection[48]. These results demonstrate that 19RS strains contain novel IS256 insertions not found in WT *E. faecalis* V583. These results also suggest that 19RS strains, even though they were isolated as individual colonies, are heterogeneous populations with varied abundances of IS256 insertions.

To determine the global effect of IS256 transposition in the 19RS strains, we performed Southern blotting using a probe against IS256 (Fig. 3C). We found differential IS256 banding patterns in the 19RS strains that are not found in WT *E. faecalis* V583, demonstrating that phage infection modulates IS256 transposition. To test if IS256 provides an advantage to *E. faecalis* against phage infection, we transformed a multi-copy plasmid containing either an IS256 gene or an inactive IS256 gene lacking the coding sequences for the two catalytic aspartic acid residues of the Tnp's DDE motif into *E. faecalis* OG1RF, which lacks native IS256 and infected these cells with phi19 (Fig. 3D). We found that cells containing a functional IS256 gene were more resistant to phage infection compared to cells containing the catalytically dead Tnp or the empty vector, indicating that IS256 carriage increases mutation frequency. To understand if IS256 activation was initiated by phi19 infection, we quantified the number of IS256 circular intermediates. IS256 elements circularize during transposition, which can be used to measure active transposition[30, 31]. During the course of phi19 infection, IS256 circular intermediates significantly increased relative to a mock-infected cells (Fig. 3E).

Southern blotting and WGS analysis indicate that phage predation increases IS256 expansion across the *E. faecalis* genome. However, these methods are low resolution. To quantify the exact locations and abundances of IS256 insertions following phage pressure, we performed IS-Seq on 19RS strains and compared these to WT *E. faecalis* V583 (Fig. 4A). IS-Seq revealed a genome-wide expansion of IS256 insertions at new locations in 19RS strains (Fig. 4A). Pairwise comparisons determined that 19RS strains are significantly enriched in the number of novel IS256 insertions compared WT *E. faecalis* V583 (Figure 4B & Table S2). New IS256 insertions in the pTEF plasmids were also found in the 19RS strains (Fig. S3A-C). Additionally, we measured IS256 circular intermediates in our IS-Seq dataset by aligning IS256 reads (which originate from the left terminus of IS256) to the right terminus of an IS256 element. We found that 19RS strains have a significantly greater number of IS256 circular intermediates compared to WT *E. faecalis* V583 (Fig. 4C).

We focused on two genomic regions that experienced a high level of IS256 insertions in the 19RS strains. The first was the *epa* locus. In addition to numerous novel insertions in *epaX*, we found insertions within other *epa* genes including *epaR*, *epaS*, *epaAA* and *epaAB*. (Fig. S4A). IS256 insertions in these *epa* genes would alter the teichoic acid decoration of the core rhammnose-containing Epa, likely altering the surface chemistry of *E. faecalis* and rendering them resistant to phage infection[18]. We also identified multiple insertions in the *vex/vnc* operon (Fig. S4B), which is purported to have both virulence and antibiotic resistance functions[55, 56].

*E. faecalis* is a native member of the intestinal microbiota and can outgrow and cause disease during intestinal dysbiosis. Phages have been proposed as a treatment option for difficult to control enterococcal intestinal blooms[57]. To determine if phage predation supported IS256 expansion in the intestine, we colonized mice with *E. faecalis* V583 and orally challenged these animals with phi19 (Fig. S5). We performed IS-Seq on fecal gDNA from these animals and found that phi19 exposure in the intestine also increased new IS256 insertions, albeit to a lesser extent than in vitro (Fig. 4D-F, Fig. S3D-F, & Table S3). We found that similar to cells

exposed to phi19 in vitro, IS256 insertions within the same location in *epaX* and the *vex*/*vnc* operons are observed in the mouse intestine following phage administration (Fig. S4C-D). This suggests that phage selection plays a role in IS256 expansion with the context of the native intestinal habitat.

***Enterococci with expanded IS256 genomes chronically shed phi19 phages.***

Phages can lysogenize their host bacterium[58]. During lysogeny the phage genome is maintained in a dormant state as an integrated element within the bacterial chromosome or as a cytoplasmic episome. Episomal phage genomes can also be in an intermediate state between lytic replication and lysogenic conversion referred to as a pseudolysogen or carrier state. Such phages can enter the lytic cycle spontaneously or following cell stress, and reports indicate that lysogenic phages can be continuously shed from cells with little to no reduction in viability of the overall bacterial population[59, 60]. During the analysis of bacterial colonies originating from *E. faecalis* 19RS strains, we discovered that the phi19 genome is maintained in these phage-resistant bacteria, and is not integrated in the bacterial chromosome. This carriage of the phi19 genome may explain its ability to influence IS256 transposition. We found that 19RS strains continually release infectious phage particles with little impact on the viability of the bacterial population (Fig. 5A). These particles were confirmed to be phi19 using PCR (Fig. 5B). We discovered that ~10% of 19RS colonies produced infectious phages (Fig. 5C). This suggests that a minority of each population exerts a selective pressure to maintain phage resistance by producing infectious phage progeny. Loss of phage resistance in this population would lead to phage infection and population collapse. Colonies that produced zones of clearing were isolated and serially passaged for three passages. All cells that initially produced zones of clearing continued to produce zones for all three passages (Fig. S6), demonstrating that phi19 is stably carried in this subpopulation of cells. Finally, we reanalyzed reads from our WGS experiments and found that we could recover the phi19 genome with high coverage from 19RS strains (Fig.

5D). Wild type *E. faecalis* V583 did not have any detectable phi19 genomic DNA. Collectively, these results show that 19RS strains release phages from a subpopulation of cells, which may impose stress on *E. faecalis* influencing IS256 expansion.

Considering that 19RS strains have IS256-rich genomes and release infectious phages, we hypothesized that phage carriage may increase the competitiveness of these 19RS strains when co-cultured with phage sensitive strains. We performed competition assays where *E. faecalis* V583 WT or 19RS strains were competed against *E. faecalis* OG1RF, which is sensitive to phi19 infection, or an OG1RF Δ*epaOX* mutant strain (homologous to *E. faecalis* V583 *epaX*) [61] that is resistant to phi19 infection, without the addition of exogenous phages to the cultures (Fig. 6). 19RS strains that were shedding phi19 outcompeted WT *E. faecalis* OG1RF. However, they were unable to outcompete *E. faecalis* OG1RF Δ*epaOX*. These results demonstrate that phi19 carriage provides a selective advantage to *E. faecalis* cells when competing with related bacteria that are phage susceptible but if competitors are phage resistant, phi19 carriage comes with a significant fitness cost.

***IS256 expansion occurs in enterococcal genomes during human infection.***

IS elements contribute to genome diversification and adaptive plasticity that is important for bacterial evolution[62]. Environmental pressure is a strong driver of IS element mobility[63, 64, 65], and the work described here expands this knowledge to phage predation. Antibiotics are a strong selective pressure that can promote bacterial evolution, and IS256 insertions have been tied to pathoadaptation in enterococci during human infections[36]. To assess if environmental cues such as antibiotics may be driving IS element mobility, we investigated whether enterococcal populations within a single individual infected with *E. faecium* experience IS256 expansion during therapeutic intervention. Stools samples were collected at various timepoints over 109 days, during which the individual was treated with regimens containing daptomycin, vancomycin, and the vancomycin analogue oritavancin for recurrent *E. faecium* bacteremia. IS-

Seq was performed on these samples across the time series described above (Fig. 7A). Nearly all of the insertions found using IS-Seq occurred in contigs which were likely generated from *E. faecium*, rather than *E. faecalis* (Fig. S7). We found that these *E. faecium* populations had a major expansion of IS256 insertions following oritavancin therapy compared to daptomycin and/or vancomycin therapy. Comparing differentially abundant insertions between vancomycin-containing and oritavancin treatment revealed multiple enriched insertions in the coding sequences of a putative Rib transcriptional regulator, and the *vex*/*vncRS* operon also identified as a IS256 insertion hotspot in *E. faecalis* 19RS strains (Fig. 7B-C). These two operons are likely involved in antibiotic resistance and virulence in *E. faecium* and IS256 insertions likely render these genes nonfunctional. These insertions increase in sequencing depth during the course of treatment and peak during oritavancin administration. The *vex*/*vncRS* operon in *E. faecalis* V583 contains an IS element belonging to the ISL3 family[26], indicating that the genome evolution of *E. faecium* during blood stream infection may follow a similar trajectory to *E. faecalis* V583[26]. We also found that IS256 regularly interrupts an aminoglycoside resistance operon (Fig. S8). Oscillating insertions both in coding and non-coding regions in this operon suggest that this region may be an IS256 insertion hotspot. Lastly, we found that oritavancin-treated samples had an increase in IS256 circle formation indicating that in addition to novel insertion events, active IS256 transposition is occurring during blood stream infection (Fig. 7D). Overall, these findings suggest that IS256 transposition is frequent in the intestine during *E. faecium* infection, and this transposition likely impacts the antibiotic resistance and virulence profiles of the infecting bacterial population.

## Discussion

IS elements directly shape bacterial physiological responses involved in antibiotic resistance and virulence, and are key drivers of bacterial genome evolution[66, 67, 68]. Considering the importance of IS element biology to bacterial fitness, the selective pressures that guide IS

element regulation and mobility remain poorly defined. Using the Gram-positive opportunistic pathogen *E. faecalis,* we extend our knowledge of IS elements by detailing the population biology, regulation, and expansion dynamics of IS256. IS256 is a widely distributed IS element in Gram-positive pathogens. Through the use of traditional bacterial genetics, comparative genomics, and IS-Seq we have revealed that the dynamics of IS256 insertion events are strongly dictated by phage predation and the mammalian host environment. Together these results suggest that IS256 mobility creates a genetically flexible genome that enables enterococci to rapidly adapt to diverse environmental conditions.

IS256 is common in *E. faecalis* genomes and is found more frequently in hospital adapted lineages (Fig. 1). Consistent with this idea, IS256 element abundance is a defining feature of hospital adapted *E. faecium* isolates[43, 44]. Movement of IS elements between cells requires other mobile elements, such as phages and plasmids, as IS elements lack any transforming or transducing ability[27]. The pattern of intermittent IS256 abundance in the enterococci is likely due to periodic exposure to IS256-containing mobile elements. In other words, genetically-related strains may interact with IS256-containing mobile elements at different rates, resulting in the dissemination of IS256 to only a subset of the population. The enrichment of IS256 among hospital adapted strains may reflect the need for increased genomic plasticity in these strains as they adapt to an altered host environment[44, 69]. Pathogens can utilize IS elements to form pseudogenes and to condense genome size through IS-mediated recombination, which can inhibit immune detection through loss of virulence factors and reduces the genome's metabolic burden[68, 69].

Regulation of IS256 has not been investigated in the enterococci and is key to understanding this element's biology. Here we show that IS256 is basally active in *E. faecalis* V583, yet it can be regulated at both the transcriptional and translational level (Fig. 2B-D). This is important because overactive IS256 could be catastrophic to *E. faecalis* viability and layers of regulation likely temper the elements activity until appropriate conditions require IS256

activation. Additionally, we show that IS256 has two different TSSs as part of this regulation and that both sites are regulated by asRNAs. The protein product occurring from the site-2 TSS is predicted to be truncated and it is unknown if this IS256 variant would be active. Other IS elements encode two or more protein coding frames and these different protein products can contribute to IS element regulation through inhibition[67, 70]. Using IS-Seq as a readout of basal IS256 mobility, we show that IS256 insertions function as a mechanism of genome-wide mutation (Fig. 2A). This is the highest resolution IS-Seq map created, to our knowledge, and demonstrates that this technique can identify low-abundance insertions with high confidence[50, 51]. Baseline IS256 movement likely adds mutational diversity to an enterococcal population which allows for adaption to changing environmental conditions through selection.

Previous work from our group determined that *E. faecalis* infection by the phage phi19 was associated with an expansion of IS256 insertions[18] (Fig. 3A). This was found using WGS that was based on less than 10 reads per insertion. We extended this observation by performing IS-Seq to accurately identify these novel insertion sites both in vitro and in vivo. We found that *E. faecalis* challenged with phi19 (19RS strains) had a major increase in new IS256 insertions (Fig. 4A-B). 19RS strains were chronically infected by phi19 and cells within the population carried the phi19 genome and this chronic infection may provide a continuous selective pressure that aids in IS256 mobility. This correlated with 19RS strains harboring elevated IS256 circularization intermediates (Fig. 4C). These circles are formed during IS256 copy-paste transposition and have been studied extensively[30].

We also observed that in a mouse model of *E. faecalis* V583 intestinal colonization, exposure to phi19 resulted in a similar expansion of IS256 (Fig. 4D-F). IS256 expansion was less robust in the mouse intestine compared to the levels of expansion seen in vitro. This may be for several reasons, including a lower frequency of insertion events per location in vivo and a lower number of samples sequenced. An additional explanation is that Epa is crucial for

bacterial colonization and *epa* mutations may lead to these mutants being outcompeted in the intestine[18, 71].

Although we found evidence for phage-mediated IS256 activation in *E. faecalis* 19RS strains, we also determined that selection is important for the location of IS256 expansion (Fig. 4G-H). Cells that were not exposed to phi19 had lower IS256 read density in *epaX*. *EpaX* is a glycosyltransferase involved in teichoic acid decoration of the core rhamnose containing Epa exopolysaccharide backbone. Mutations in *epaX* result in poor phage adsorption[18]. We found no other insertions in genes known to be involved in phage infection indicating that *epaX* and other *epa* genes are likely hotspots for IS256 integration following phage pressure. In light of these discoveries, we hypothesize that initial phage infection may select for *epa*-IS256 insertions and that prolonged phage exposure though chronic infection leads to increased and non-specific IS256 transposition as a stress response. We suspect that phage carriage and release will continually pressure intermittently resistant cells and force fully resistant cells to maintain high levels of resistance.

IS elements are involved in pseudogene formation during pathoadaption. Examples include IS256 insertions in the cytolysin operon of *E. faecalis* V583[36] and a dependence on IS insertions in *E. coli* to evolve resistance to macrophage killing[72]. Additionally, how enterococci evolve during human infection is not well understood and may involve a variety of genetic changes in cell wall modifying[73] and cellular respiration[74] genes. While IS elements are directly involved in enterococcal pathoadaptation [36], an in-depth analysis of IS-mediated mutations during human infection had never been performed. Previously, such dynamics were studied by laboriously sequencing individual isolates. While this approach can successfully identify new IS element insertion sites, it overlooks IS element mobility within the entirety of the bacterial population. Here, we show that IS-Seq can be used to study bacterial pathoadaptation at the population level and can reveal multiple pathogen-associated insertions within such a population (Fig. 7). Following oritavancin therapy an increase in IS256 insertions occurred in the

413 *vex*/*vncRS* operon, which has been implicated in both virulence[56] and vancomycin resistance[55].
414 Additionally, there is an increase in insertions in a putative transcriptional regulator that may
415 regulate a Rib/Alpha adhesin[75, 76]. Loss of these potential virulence factors may lead to
416 modulation of virulence and avoidance of immune activation or detection. Additionally, we found
417 highly abundant IS256 insertions in an aminoglycoside acetyltransferase. Vancomycin is
418 reported to act synergistically with gentamicin against enterococci[77], likely due to increased
419 gentamicin transport through the vancomycin-permeabilized cell wall[78]. In recent years,
420 enterococci with aminoglycoside resistance have emerged[79] with acquisition of resistance
421 genes carried in an IS256 composite transposon[80]. Our results suggest that genetic modulation
422 of aminoglycoside resistance fluctuates in the host during infection, with different highly
423 abundant insertions prominent at different timepoints. This data suggests that aminoglycoside
424 resistance is repeatedly modulated and the intestinal enterococcal population regularly samples
425 different versions of this aminoglycoside resistance operon. Future studies to identify if
426 glycopeptide treatment potentiates aminoglycoside sensitivity through IS256 insertions is
427 warranted. We additionally show that oritavancin treatment is associated with IS256 expansion
428 in this patient. Oritavancin is an analog of vancomycin, but is also reported to disrupt cell
429 membrane integrity and possess additional mechanisms for inhibiting cell wall synthesis[81]. This
430 may explain the difference in IS256 expandability, as this antibiotic may impose stronger
431 pressure resulting in a broader range of mutations. Likewise, oritavancin treatment was
432 associated with an increase in IS256 circles. In *Staphylococcus aureus*, vancomycin treatment
433 increases IS256 transposition[35, 82], reflecting a similar glycopeptide-induced IS256 activation.
434 In summary, we show how the widespread and clinically-relevant IS element IS256
435 creates genome diversification during phage predation and human infection using sensitive
436 NGS IS-Seq. This work provides a high-resolution picture of IS256 movement during both
437 steady-state and stress inducing conditions. Understanding the outcomes of these IS256
438 insertion events will be critical to the study of the evolution of enterococcal pathogenesis in

response to both phage and antibiotic therapies. We also show that IS256 is regulated at both the transcriptional and translational level in *E. faecalis* and have discovered that IS256 mobility is biased for highly mobilizable insertion events in nosocomial and virulent enterococcal isolates, further demonstrating that IS elements are domesticated and specialized in their choice of bacterial host.

## Materials and Methods

*Bacteria and bacteriophages.*

*E. faecalis* strains were grown in BHI broth with aeration at 37°C. A list of bacterial and bacteriophage strains can be found here (Table S4). *Escherichia coli* cultures were grown in Lennox L broth at 37°C with aeration. 15 µg/mL or 5 µg/mL chloramphenicol was used for selection of transformed *E. coli* and *E. faecalis*, respectively. The generation of phage-resistant 19RS strains was recently described[18].

*Enterococcal phylogeny and Identification of IS256 in enterococcal genomes*

All available *E. faecalis* and *E. faecium* genomes were downloaded from NCBI RefSeq on 3/21/2022. Phylogenetic tree was constructed with GToTree v1.6.31 using default parameters[83], pruned using treeshrink v1.3.9[84], and visualized using the iTOL viewer[85]. IS256 transposase genes were identified using GToTree with the IS256 pfam “PF00872” and 100% amino acid matches to the IS256 Tnp from *E. faecalis* V583 were found using seqkit v0.16.1[86].

*MLST and virulence factor abundance*

*Enterococcal* genomes obtained from RefSeq were assigned an MLST type using mlst v2.19.0[87] with the *E. faecalis* and *E. faecium* MLST scheme from pubmlst[88]. Virulence factors were identified by calling all predicted ORFs in all downloaded RefSeq genomes using prodigal v2.6.3[89] and running diamond blastp v0.9.21[90] against this database with known *E. faecalis* and

*E. faecium* virulence factors from the Virulence Factor Database[91]. All further analyses and statistics were performed in R.

*DNA extraction and IS-Seq*

Bacterial genomic DNA was extracted from overnight cultures grown in 5 mL BHI broth using the Zymo BIOmics DNA Miniprep Kit (Zymo, Irvine, CA). For library preparation, 200 ng of genomic DNA was used as input in the Illumina DNA Prep Kit following the manufacturer's instructions (Illumina, San Diego, CA). Following library construction, IS256 enrichment was performed as follows. First, 10 ng of library DNA was amplified with the p7 primer and the IS-Seq Step1 primer (Table S5) for 13 cycles using Q5 2X Master Mix (NEB, Ipswich, MA). The products of this reaction were diluted 1:100 and 10 µL was added to a PCR reaction with the p7 primer and the IS-Seq Step2 primer for 9 cycles using Q5 2X Master Mix. The products of this second reaction were sequenced on an Illumina NovaSEQ 6000 by the University of Colorado Anschutz Medical Center Genomics Core with paired-end 150 cycle chemistry. 23.3 ± 3.8 M reads, 17.9 ± 2.5 M reads, and 16.3 ± 2.6 M reads were obtained from sequencing the human, mouse, and *in vitro* IS-Seq libraries, respectively. IS-seq reads have been deposited in the European Nucleotide Archive under project accession number PRJEB55280.

*IS-Seq analysis*

Paired end reads obtained from IS-Seq were partitioned into read1 and read2 files, and reads from read1 files were used in the downstream analysis. First, cutadapt v1.18 was used to bin reads with a full IS256 5' terminus. the IS256 5' terminus was then trimmed from these reads[92] suing cutadapt with the following flags: '-O 6 -g "^CGTAAAAGGACTGTTATATGGCCTTTTTACTTTTACACAATTATACGGACTTTATC" '. These trimmed reads were aligned to the *E. faecalis* V583 chromosome using Bowtie2 v2.3.5.1[93] and the location of each insertion was determined using samtools v1.13[94] and

bedtools genomecov v2.30.0[95]. All downstream analysis was performed in R. Insertion site abundances were normalized using DESeq2 estimateSizeFactors[96] and significantly enriched unique insertion sites were found using DESeq2. Both significantly enriched and insignificant insertions with at least 100 reads were reported in tables and figures.

*E. faecalis phi19 infection in the mouse intestine*

All animal protocols were approved by the Institutional Animal Care and Use Committee of the University of Colorado School of Medicine (protocol number 00253). Conventional 6-week-old C57BL/6 mice were divided into two groups (Control: 2 female/2 male, Experimental: 2 female/2male). All mice were treated with an antibiotic cocktail (streptomycin [1 mg/ml], gentamicin [1 mg/ml], erythromycin [200 µg/ml]) by first dosing via oral gavage with 100 µl of the cocktail and replacing their drinking water with the same antibiotic cocktail for 1 week. On day 7, water bottles were replaced with antibiotic free-drinking water. After 24 hours mice were colonized with *E. faecalis* V583 suspended in phosphate buffered saline (PBS) by oral gavage ($10^9$ CFU in 100 µl). After 24 hours mice were orally gavaged daily as follows: 100 µl of 1M sodium bicarbonate (all mice) and 100 µl PBS per control mouse or $10^9$ PFU phi19 in 100 µl per experimental mouse. Feces were collected daily and homogenized in 1ml PBS. 10µl of the fecal slurry was serially diluted and plated on BHI agar containing 100 µg/ml gentamicin or 100 µg/ml gentamicin and $10^8$ pfu/ml phi19. From the experimental samples, 5 µl of slurry was mixed with 45µl chloroform, spun at 16,363 RCF for 1 min and the supernatant was enumerated for phage particles by agar overlay plaque assay as described previously[19].

*RNA extraction and qPCR*

RNA was isolated from logarithmically growing (OD=0.3) *E. faecalis* using a modified protocol for the RNeasy Mini-Prep Kit (Qiagen, Hilden, Germany). First, cell pellets were collected by centrifugation of 5 mL of cell culture at 8,228 RCF for 5 minutes. Cell pellets were

517 resuspended in 1 mL RNAlater and centrifuged again at 8,228 RCF for 10 minutes. The cell
518 pellets were stored at -80 C until sample processing. To isolate RNA, the pellets were thawed
519 and resuspended in 100 µL TE buffer with 15 mg/mL lysozyme and incubated at room
520 temperature for 30 minutes. Following this, 700 µL Buffer RLT with 0.01% beta-mercaptoethanol
521 was added and the sample was transferred to a Lysing Matrix B tube (MPBio, Irvine, CA). The
522 tubes were bead-beaten in a Mini-Beadbeater-16 (Biospec Products, Bartlesville, OK) on the
523 fastest setting at 30-second intervals with 1 minute rests on ice between cycles. Following bead
524 beating, the supernatant was removed after centrifugation at 16,363 RCF for 30 seconds and
525 processed following the manufacturer's instructions. RNA was eluted from the column in
526 RNase/DNase free $H_2O$ and any residual DNA contamination was removed with a 1 hour off-
527 column DNase treatment (Qiagen). The RNA was purified following the RNeasy Mini-Prep Kit
528 following manufacturer's instructions. cDNA was synthesized using Qscript Master Mix
529 (Quantabio, Beverley, MA) and 1 µg RNA. For qPCR of gDNA targets, 1 ng of gDNA template
530 was used per reaction. qPCR was run with PowerUp SYBR Green Master Mix (Thermo Fisher,
531 Waltham, MA) on an Applied Biosystems QuantStudio 7 Flex qPCR system. qPCR primers are
532 listed in Table S5.
533
534 *DNA manipulation and cloning*
535 All cloning primers and DNA constructs used in this study are listed in Table S5. All
536 plasmid constructs used the pLZ12 shuttle vector backbone[97]. For cloning, all inserts were
537 amplified using 2X Q5 DNA polymerase Master Mix and assembled using 2X Gibson Assembly
538 Master Mix (NEB).
539
540 *Phage carriage identification and serial passaging*
541 To enumerate extracellular viral particles, we collected supernatant from cultures after
542 centrifugation for 1 minute at 10,000 RCF, treated with 1/10 volume chloroform, centrifuged for

1 min at 21,000 RCF and extracted the aqueous phase. The resulting supernatant was serially diluted in SM+ buffer (50 mM Tris-HCl, 100 mM NaCl, 8 mM $MgSO_4$, 5 mM $CaCl_2$ [pH 7.4]), and 10 µL was mixed with 130 µL of a 1:10 dilution of *E. faecalis* V583 cells grown overnight. This mixture was combined with 5 mL of 0.35% Todd Hewitt agar (THA) supplemented with 10mM $MgSO_4$, and poured onto THA+10mM $MgSO_4$ plates.

To identify 19RS *E. faecalis* cells actively shedding phages, glycerol stocks of phage-resistant cultures were streaked on BHI agar and incubated at 37°C. After overnight growth, 182 µL of a 1:10 dilution in SM+ of an overnight wild type *E. faecalis* V583 culture was mixed with 7 mL of 0.35% Todd Hewitt agar (THA) and 10mM $MgSO_4$ and solidified on THA+10mM $MgSO_4$ plates for 30 minutes. Individual colonies were picked from the overnight plate patched onto the plate containing *E. faecalis* V583 embedded in 0.35% THA, with care not to break the surface of the agar, and incubated at 37°C overnight.

To serially passage phage-positive colonies, colonies producing zones of clearing were patched onto both THA+10mM $MgSO_4$ plates and THA+10mM $MgSO_4$ with an *E. faecalis* V583 top agar layer as described above. The next day, the colony on the THA+10mM $MgSO_4$ plate was patched onto both types of plates and this was continued for two subsequent passages.

*Competition assays*

*E. faecalis* cultures were grown overnight in BHI broth and diluted to an $OD_{600}$ of 1 in PBS. 30 µL of each strain was added to 3 mL BHI and incubated at 37°C for 24 hours. The cultures were plated on both BHI gentamicin 100 µg/mL to select for *E. faecalis* V583 strains and BHI rifampicin 25 µg/mL, fusidic acid 50 µg/mL to select for *E. faecalis* OG1RF or E. faecalis OG1RF Δ*epaOX*.

*Enterococcal isolation from stool samples and gDNA extraction*

Enterococcal stool populations were obtained over a span of 109 days from a patient being treated for recurrent *E. faecium* bacteremia. Stool samples were diluted and plated onto bile esculin azide – Enterococcosel agar (Becton Dickinson, Franklin Lakes, NJ), and 100-1,000 colonies were collected and pooled into BHI containing 16.7% glycerol and stored at -80°C. One mL aliquots of the frozen population stocks were thawed and washed with BHI. Populations were allowed to briefly expand at 37°C at 170 rpm for 5.5 hours. The cultures were pelleted and genomic DNA was extracted into DNase free water using the DNeasy Blood and Tissue Kit (Qiagen). gDNA concentrations were determined with the Qubit 1X dsDNA High-Sensitivity Kit and fluorometer (Invitrogen, Thermo Fisher).

*Statistics and Visualization*

Graphs were made in Graphpad Prism or in R using dplyr and ggplot2. T-tests and one-way ANOVAs were calculated in Graphpad Prism and insertion site differential abundance and proportional tests (prop.test) were calculated in R.

**Acknowledgements**

This work was supported by National Institutes of Health grants R01AI141479 (B.A.D.), R01AI165519 (D.V.T.), R01AI116610 (K.L.P.), T32AI052066 (J.M.K), F31AI169976 (J.M.K.), and T32AI138954 (M.E.S.).

**Figure Legends**

**Figure 1. Distribution of IS256 in *E. faecalis* and *E. faecium.* A)** Phylogenetic tree of *E. faecalis* genomes. Genomes with IS256 are labeled in red and genomes without IS256 are labeled in black. **B)** Presence or absence of IS256 in the genomes of hospital adapted *E. faecalis* MLST types. **C)** Comparison of *E. faecalis* virulence factor abundances in the genomes of hospital adapted *E. faecalis* MLST types. **D)** Phylogenetic tree of *E. faecium genomes*.

Genomes with IS256 are labeled in red and genomes without IS256 are labeled in black. **E)** Presence or absence of IS256 in the genomes of hospital adapted *E. faecium* MLST types. **F)** Comparison of *E. faecium* virulence factor abundances in the genomes of hospital adapted *E. faecium* MLST types. **G)** Percent of *E. faecalis* and *E. faecium* genomes from RefSeq that contain IS256. (* $p<0.05$, ** $p<10^{-5}$, *** $p<10^{-25}$, determined with chi-squared test)

**Figure 2. Regulation of IS256 Tnp activity during steady state conditions. A)** IS256 sequencing (IS-Seq) from three individual *E. faecalis* V583 cultures. Peaks indicated in black represent the six endogenous IS256 insertions identified in the sequenced genome of V583. **B)** qPCR of IS256 *tnp* gene expression relative to the housekeeping protease gene *clpX*. **C)** Stranded RNA-Seq of IS256 tnp gene expression in *E. faecalis* V583. **D)** IS256 Tnp protein expression indicated by measuring GFP fluorescence of an IS256-GFP and IS256-GFP ΔasRNA translational fusions. (* $p<0.05$, determined with multiple t-tests)

**Figure 3. IS256 expansion confers phage resistance and is elevated in *E. faecalis* isolates resistant to phi19. A)** Enumeration of predicted IS256 insertions determined from whole genome sequencing of *E. faecalis* phage resistant 19RS strains. **B)** PCR showing that IS256 insertions occur in both the positive and negative strand orientations in the *epaX* gene 19RS strains. **C)** Southern blot analysis of global IS256 insertions in wild type (WT) *E. faecalis* V583 and 19RS strains. Red arrows indicate novel IS256 banding patterns. **D)** Emergence of phage resistant *E. faecalis* OG1RF with IS256 or a catalytically dead (ΔDDE) IS256. EV indicates *E. faecalis* OG1RF carrying the empty vector. **E)** qPCR quantification of IS256 circular intermediates normalized to total cell density following phi19 infection or mock infection (MI). (* $p<0.05$, ** $p<0.01$, determined with multiple t-tests).

**Figure 4. IS-Seq to identify IS256 insertion sites in *E. faecalis* phage resistant isolates in vitro and in vivo. A)** IS-Seq of *E. faecalis* V583, and 19RS strains. **B)** Quantification of significantly enriched insertions between pairwise comparisons of each group in A. In each

square, the top value is the number of insertions overabundant in the column group and the bottom value is number of insertions overabundant in the row group. **C)** IS256 circle formation determined with IS-Seq from samples shown in A. **D)** IS-Seq of E. faecalis V583 and phage resistant colonies isolated from the feces of mice colonized with (Mouse 5 & 6) and without (Mouse 1 & 2) oral phi19 inoculation. **E)** Quantification of significantly enriched insertions between pairwise comparisons of each group in D. In each square, the top value is the number of insertions overabundant in the column group and the bottom value is number of insertions overabundant in the row group. **F)** IS256 circle formation determined with IS-Seq from samples shown in D.

**Figure 5. *E. faecalis* 19RS strains chronically shed phi19 virus and harbor the phage genome intracellularly. A)** Quantification of shed infectious phi19 phage particles. **B)** PCR confirmation of phi19 recovered from culture fluid of *E. faecalis* 19RS strains. **C)** Proportion of cells actively replicating and releasing infectious phi19 phage particles. **D)** WGS read mapping alignments to the phi19 genome from *E. faecalis* V583 and 19RS strains.

**Figure 6. phi19 shedding *E. faecalis* 19RS strains are more fit during competition with a phage susceptible *E. faecalis* strain.** Competitive fitness of *E. faecalis* V583 and 19RS strains relative to *E. faecalis* OG1RF or an *E. faecalis* OG1RF derivative with a deletion in the *epaX* homolog *epaOX*.

**Figure 7. IS-Seq of a longitudinal series stool samples from a human patient with a vancomycin resistant enterococcal infection. A)** Insertions found via IS-Seq plotted on a concatenated “metagenome” of contiguous enterococcal sequences from stool genomic DNA. IS256 sequences were mapped against individual contigs to identify IS256 insertion locations. Then all contigs were concatenated together to build a linearized representation of the metagenome. **B)** Volcano plot of differentially abundant insertions during Daptomycin+Vancomycin co-therapy and Oritavancin therapy. Enriched insertions (dark red)

were overabundant during Oritavancin therapy. **C)** Gene organization of loci where elevated IS256 insertions occurred are indicated by arrows. Lollipops show the location of IS256 insertion and bar graphs are read depth abundances found for each insertion. (* $p< 0.05$, **, $p< 0.01$, ***, $p< 0.001$, determined with DESeq2) **D)** IS256 circle formation for each treatment group inferred from IS-Seq.

**Figure S1. Enrichment of IS256-chrmosomal junctions during IS-Seq. A)** Schematic of the IS-Seq PCR amplification step. **B)** Trimming site and binning strategy used to identify IS256-termini reads.

**Figure S2. Steady state IS256 insertion sites in the native *E. faecalis* V583 plasmids. A)** pTEF1, **B)** pTEF2, and **C)** pTEF3.

**Figure S3. IS256 insertions in *E. faecalis* V583 plasmids in vitro and in vivo. A-C)** Insertion sties from in vitro cultured *E. faecalis* 19RS strains; **A)** pTEF1, **B)** pTEF2, and **C)** pTEF3. **D-F)** Insertion sites from *E. faecalis* isolated from the murine intestine **D)** pTEF1, **E)** pTEF2, and **F)** pTEF3.

**Figure S4. IS-256 insertions in *epa* and *vex*/*vnc* genes in vitro and in vivo.** Insertion sties from in vitro cultured *E. faecalis* 19RS strains in the **A)** *epa* locus and **B)** *vex*/*vnc* locus. Insertion sites from E. faecalis isolated from the murine intestine in the **C)** *epa* locus and **D)** *vex*/*vnc* locus.

**Figure S5. Murine model and intestinal *E. faecalis* colonization and oral phi19 treatment. A)** Schematic of the *E. faecalis* intestinal colonization model used to identify in vivo IS256 mobilization. **B)** Colony forming units of *E. faecalis* isolated from mouse feces. Bacteria were enumerated on growth media supplemented with gentamicin with and without the addition of phi19 to measure the frequency of phage resistant colonies. Arrows indicate time points where IS-Seq was performed.

**Figure S6. Serial passage of phi19 shedding *E. faecalis* 19RS isolates.**

**Figure S5. IS256 read mapping to enterococcal genomic contigs assembled from stool samples.** Each data point indicates the read mapping abundance per assembled contig. Data points indicated as *E. faecalis* or *E. faecium* lacked sufficient data to definitively categorize these contigs as either *E. faecalis* or *E. faecium*.

**Figure S8. IS256 insertions from human stool enterococcal isolates in genes involved in aminoglycoside resistance.**

## References

1. Fiore E, Van Tyne D, Gilmore MS. Pathogenicity of enterococci. *Microbiol Spectr* **7**, (2019).

2. Shah ASV*, et al.* Incidence, microbiology, and outcomes in patients hospitalized with infective endocarditis. *Circulation* **141**, 2067-2077 (2020).

3. Khan A, Aslam A, Satti KN, Ashiq S. Infective endocarditis post-transcatheter aortic valve implantation (TAVI), microbiological profile and clinical outcomes: A systematic review. *PLoS One* **15**, e0225077 (2020).

4. CDC. 2019 AR Threats Report.) (2019).

5. Markwart R*, et al.* The rise in vancomycin-resistant *Enterococcus faecium* in Germany: data from the German Antimicrobial Resistance Surveillance (ARS). *Antimicrob Resist Infect Control* **8**, 147 (2019).

6. Cetinkaya Y, Falk P, Mayhall CG. Vancomycin-resistant enterococci. *Clin Microbiol Rev* **13**, 686-707 (2000).

7. Partridge SR, Kwong SM, Firth N, Jensen SO. Mobile genetic elements associated with antimicrobial resistance. *Clin Microbiol Rev* **31**, (2018).

8. Schwarz FV, Perreten V, Teuber M. Sequence of the 50-kb conjugative multiresistance plasmid pRE25 from *Enterococcus faecalis* RE25. *Plasmid* **46**, 170-187 (2001).

9. Hodel-Christian SL, Murray BE. Characterization of the gentamicin resistance transposon Tn5281 from *Enterococcus faecalis* and comparison to staphylococcal transposons Tn4001 and Tn4031. *Antimicrob Agents Chemother* **35**, 1147-1152 (1991).

10. Arthur M, Molinas C, Depardieu F, Courvalin P. Characterization of Tn1546, a Tn3-related transposon conferring glycopeptide resistance by synthesis of depsipeptide peptidoglycan precursors in *Enterococcus faecium* BM4147. *J Bacteriol* **175**, 117-127 (1993).

11. Quintiliani R, Jr., Courvalin P. Characterization of Tn1547, a composite transposon flanked by the IS16 and IS256-like elements, that confers vancomycin resistance in *Enterococcus faecalis* BM4281. *Gene* **172**, 1-8 (1996).

12. Kortright KE, Chan BK, Koff JL, Turner PE. Phage therapy: a renewed approach to combat antibiotic-resistant bacteria. *Cell Host Microbe* **25**, 219-232 (2019).

13. Chan BK, Turner PE, Kim S, Mojibian HR, Elefteriades JA, Narayan D. Phage areatment of an aortic graft infected with *Pseudomonas aeruginosa*. *Evol Med Public Health* **2018**, 60-66 (2018).

14. Schooley RT*, et al.* Development and use of personalized bacteriophage-based therapeutic cocktails to treat a patient with a disseminated resistant *Acinetobacter baumannii* infection. *Antimicrob Agents Chemother* **61**, (2017).

15. Dedrick RM*, et al.* Engineered bacteriophages for treatment of a patient with a disseminated drug-resistant *Mycobacterium abscessus*. *Nat Med* **25**, 730-733 (2019).

16. Aslam S*, et al.* Lessons learned from the first 10 consecutive cases of intravenous bacteriophage therapy to treat multidrug-resistant bacterial infections at a single center in the United States. *Open Forum Infect Dis* **7**, ofaa389 (2020).

17. Petrovic Fabijan A, Lin RCY, Ho J, Maddocks S, Ben Zakour NL, Iredell JR. Safety of bacteriophage therapy in severe *Staphylococcus aureus* infection. *Nat Microbiol* **5**, 465-472 (2020).

18. Chatterjee A*, et al.* Bacteriophage resistance alters antibiotic-mediated intestinal expansion of enterococci. *Infect Immun* **87**, (2019).

19. Duerkop BA, Huo W, Bhardwaj P, Palmer KL, Hooper LV. Molecular basis for lytic bacteriophage resistance in enterococci. *mBio* **7**, (2016).

20. Markwitz P, Lood C, Olszak T, van Noort V, Lavigne R, Drulis-Kawa Z. Genome-driven elucidation of phage-host interplay and impact of phage resistance evolution on bacterial fitness. *ISME J* **16**, 533-542 (2022).

21. Hesse S*, et al.* Phage resistance in multidrug-resistant *Klebsiella pneumoniae* ST258 evolves via diverse mutations that culminate in impaired adsorption. *mBio* **11**, (2020).

22. Woodford N, Ellington MJ. The emergence of antibiotic resistance by mutation. *Clin Microbiol Infect* **13**, 5-18 (2007).

23. Mangalea MR, Duerkop BA. Fitness trade-offs resulting from bacteriophage resistance potentiate synergistic antibacterial strategies. *Infect Immun* **88**, (2020).

24. Gordillo Altamirano F*, et al.* Bacteriophage-resistant *Acinetobacter baumannii* are resensitized to antimicrobials. *Nat Microbiol* **6**, 157-161 (2021).

25. Castledine M*, et al.* Parallel evolution of Pseudomonas aeruginosa phage resistance and virulence loss in response to phage treatment in vivo and in vitro. *eLife* **11**, e73679 (2022).

26. Paulsen IT*, et al.* Role of mobile DNA in the evolution of vancomycin-resistant *Enterococcus faecalis*. *Science* **299**, 2071-2074 (2003).

27. Johnson CN, Sheriff EK, Duerkop BA, Chatterjee A. Let me upgrade you: impact of mobile genetic elements on enterococcal adaptation and evolution. *J Bacteriol* **203**, e0017721 (2021).

28. Clewell DB, Weaver KE, Dunny GM, Coque TM, Francia MV, Hayes F. Extrachromosomal and mobile elements in enterococci: transmission, maintenance, and epidemiology. In: *Enterococci: From Commensals to Leading Causes of Drug Resistant Infection* (eds Gilmore MS, Clewell DB, Ike Y, Shankar N). Massachusetts Eye and Ear Infirmary (2014).

29. Werner G, Fleige C, Geringer U, van Schaik W, Klare I, Witte W. IS element IS16 as a molecular screening tool to identify hospital-associated strains of *Enterococcus faecium*. *BMC Infect Dis* **11**, 80 (2011).

30. Loessner I, Dietrich K, Dittrich D, Hacker J, Ziebuhr W. Transposase-dependent formation of circular IS256 derivatives in *Staphylococcus epidermidis* and *Staphylococcus aureus*. *J Bacteriol* **184**, 4709-4714 (2002).

31. Valle J, Vergara-Irigaray M, Merino N, Penadés JR, Lasa I. sigmaB regulates IS256-mediated *Staphylococcus aureus* biofilm phenotypic variation. *J Bacteriol* **189**, 2886-2896 (2007).

32. Kozitskaya S, Cho SH, Dietrich K, Marre R, Naber K, Ziebuhr W. The bacterial insertion sequence element IS256 occurs preferentially in nosocomial *Staphylococcus*

*epidermidis* isolates: association with biofilm formation and resistance to aminoglycosides. *Infect Immun* **72**, 1210-1215 (2004).

33. Kleinert F*, et al.* Influence of IS256 on genome variability and formation of small-colony variants in *Staphylococcus aureus*. *Antimicrob Agents Chemother* **61**, (2017).

34. McEvoy CR*, et al.* Decreased vancomycin susceptibility in *Staphylococcus aureus* caused by IS256 tempering of WalKR expression. *Antimicrob Agents Chemother* **57**, 3240-3249 (2013).

35. Nagel M, Reuter T, Jansen A, Szekat C, Bierbaum G. Influence of ciprofloxacin and vancomycin on mutation rate and transposition of IS256 in *Staphylococcus aureus*. *Int J Med Microbiol* **301**, 229-236 (2011).

36. Shankar N, Baghdayan AS, Gilmore MS. Modulation of virulence within a pathogenicity island in vancomycin-resistant *Enterococcus faecalis*. *Nature* **417**, 746-750 (2002).

37. Manson JM, Hancock LE, Gilmore MS. Mechanism of chromosomal transfer of *Enterococcus faecalis* pathogenicity island, capsule, antimicrobial resistance, and other traits. *Proc Natl Acad Sci U S A* **107**, 12269-12274 (2010).

38. Leavis HL, Willems RJ, van Wamel WJ, Schuren FH, Caspers MP, Bonten MJ. Insertion sequence-driven diversification creates a globally dispersed emerging multiresistant subspecies of *E. faecium*. *PLoS Pathog* **3**, e7 (2007).

39. Pöntinen AK*, et al.* Apparent nosocomial adaptation of *Enterococcus faecalis* predates the modern hospital era. *Nat Commun* **12**, 1523 (2021).

40. Dabul ANG*, et al.* Molecular basis for the emergence of a new hospital endemic tigecycline-resistant *Enterococcus faecalis* ST103 lineage. *Infect Genet Evol* **67**, 23-32 (2019).

41. Schell CM*, et al.* Detection of β-lactamase-producing *Enterococcus faecalis* and vancomycin-resistant *Enterococcus faecium* isolates in human invasive infections in the public hospital of Tandil, Argentina. *Pathogens* **9**, (2020).

42. Zaheer R*, et al.* Surveillance of *Enterococcus* spp. reveals distinct species and antimicrobial resistance diversity across a One-Health continuum. *Sci Rep* **10**, 3937 (2020).

43. Lebreton F*, et al.* Emergence of epidemic multidrug-resistant *Enterococcus faecium* from animal and commensal strains. *mBio* **4**, (2013).

44. Chilambi GS*, et al.* Evolution of vancomycin-resistant *Enterococcus faecium* during colonization and infection in immunocompromised pediatric patients. *Proc Natl Acad Sci U S A* **117**, 11703-11714 (2020).

45. Mikalsen T*, et al.* Investigating the mobilome in clinically important lineages of *Enterococcus faecium* and *Enterococcus faecalis*. *BMC Genomics* **16**, 282 (2015).

46. Perez M*, et al.* IS256 abolishes gelatinase activity and biofilm formation in a mutant of the nosocomial pathogen *Enterococcus faecalis* V583. *Can J Microbiol* **61**, 517-519 (2015).

47. Palmer KL, Daniel A, Hardy C, Silverman J, Gilmore MS. Genetic basis for daptomycin resistance in enterococci. *Antimicrob Agents Chemother* **55**, 3345-3356 (2011).

48. Lossouarn J*, et al. Enterococcus faecalis* countermeasures defeat a virulent picovirinae bacteriophage. *Viruses* **11**, (2019).

49. Dale JL*, et al.* Comprehensive functional analysis of the *Enterococcus faecalis* core genome using an ordered, sequence-defined collection of insertional mutations in strain OG1RF. *mSystems* **3**, (2018).

50. Wright MS, Mountain S, Beeri K, Adams MD. Assessment of insertion sequence mobilization as an adaptive response to oxidative stress in *Acinetobacter baumannii* using IS-seq. *J Bacteriol* **199**, (2017).

51. Reyes A*, et al.* IS-seq: a novel high throughput survey of in vivo IS6110 transposition in multiple *Mycobacterium tuberculosis* genomes. *BMC Genomics* **13**, 249 (2012).

52. Ellis MJ, Trussler RS, Haniford DB. A cis-encoded sRNA, Hfq and mRNA secondary structure act independently to suppress IS200 transposition. *Nucleic Acids Res* **43**, 6511-6527 (2015).

53. Michaux C, Hansen EE, Jenniches L, Gerovac M, Barquist L, Vogel J. Single-nucleotide RNA maps for the two major nosocomial pathogens *Enterococcus faecalis* and *Enterococcus faecium*. *Front Cell Infect Microbiol* **10**, 600325 (2020).

54. Prudhomme M, Turlan C, Claverys JP, Chandler M. Diversity of Tn4001 transposition products: the flanking IS256 elements can form tandem dimers and IS circles. *J Bacteriol* **184**, 433-443 (2002).

55. Haas W, Sublett J, Kaushal D, Tuomanen EI. Revising the role of the pneumococcal *vex-vncRS* locus in vancomycin tolerance. *J Bacteriol* **186**, 8463-8471 (2004).

56. Lee S*, et al.* Induction of the pneumococcal *vncRS* operon by lactoferrin is essential for pneumonia. *Virulence* **9**, 1562-1575 (2018).

57. Bolocan AS*, et al.* Evaluation of phage therapy in the context of *Enterococcus faecalis* and its associated diseases. *Viruses* **11**, (2019).

58. Mäntynen S, Laanto E, Oksanen HM, Poranen MM, Díaz-Muñoz SL. Black box of phage-bacterium interactions: exploring alternative phage infection strategies. *Open Biol* **11**, 210188 (2021).

59. Liu Y*, et al.* Chronic release of tailless phage particles from *Lactococcus lactis*. *Appl Environ Microbiol* **88**, e0148321 (2022).

60. Liu J*, et al.* The diversity and host interactions of *Propionibacterium acnes* bacteriophages on human skin. *ISME J* **9**, 2078-2093 (2015).

61. Dale JL, Cagnazzo J, Phan CQ, Barnes AM, Dunny GM. Multiple roles for *Enterococcus faecalis* glycosyltransferases in biofilm-associated antibiotic resistance, cell envelope integrity, and conjugative transfer. *Antimicrob Agents Chemother* **59**, 4094-4105 (2015).

62. Touchon M, Rocha EP. Causes of insertion sequences abundance in prokaryotic genomes. *Mol Biol Evol* **24**, 969-981 (2007).

63. Drevinek P*, et al.* Oxidative stress of *Burkholderia cenocepacia* induces insertion sequence-mediated genomic rearrangements that interfere with macrorestriction-based genotyping. *J Clin Microbiol* **48**, 34-40 (2010).

64. Ohtsubo Y, Genka H, Komatsu H, Nagata Y, Tsuda M. High-temperature-induced transposition of insertion elements in *Burkholderia multivorans* ATCC 17616. *Appl Environ Microbiol* **71**, 1822-1828 (2005).

65. Pasternak C, Ton-Hoang B, Coste G, Bailone A, Chandler M, Sommer S. Irradiation-induced *Deinococcus radiodurans* genome fragmentation triggers transposition of a single resident insertion sequence. *PLoS Genet* **6**, e1000799 (2010).

66. Siguier P, Gourbeyre E, Varani A, Ton-Hoang B, Chandler M. Everyman's guide to bacterial insertion sequences. *Microbiol Spectr* **3**, MDNA3-0030-2014 (2015).

67. Siguier P, Gourbeyre E, Chandler M. Bacterial insertion sequences: their genomic impact and diversity. *FEMS Microbiol Rev* **38**, 865-891 (2014).

68. Chain PS*, et al.* Insights into the evolution of *Yersinia pestis* through whole-genome comparison with *Yersinia pseudotuberculosis*. *Proc Natl Acad Sci U S A* **101**, 13826-13831 (2004).

69. Gilmore MS, Lebreton F, van Schaik W. Genomic transition of enterococci from gut commensals to leading causes of multidrug-resistant hospital infection in the antibiotic era. *Curr Opin Microbiol* **16**, 10-16 (2013).

70. Pasternak C*, et al.* ISDra2 transposition in *Deinococcus radiodurans* is downregulated by TnpB. *Mol Microbiol* **88**, 443-455 (2013).

71. Rigottier-Gois L*, et al.* The surface rhamnopolysaccharide epa of *Enterococcus faecalis* is a key determinant of intestinal colonization. *J Infect Dis* **211**, 62-71 (2015).

72. Miskinyte M*, et al.* The genetic basis of *Escherichia coli* pathoadaptation to macrophages. *PLoS Pathog* **9**, e1003802 (2013).

73. Yang Y*, et al.* Within-host evolution of a gut pathobiont facilitates liver translocation. *Nature* **607**, 563-570 (2022).

74. Van Tyne D, Manson AL, Huycke MM, Karanicolas J, Earl AM, Gilmore MS. Impact of antibiotic treatment and host innate immune pressure on enterococcal adaptation in the human bloodstream. *Sci Transl Med* **11**, (2019).

75. Kachroo P*, et al.* Integrated analysis of population genomics, transcriptomics and virulence provides novel insights into *Streptococcus pyogenes* pathogenesis. *Nat Genet* **51**, 548-559 (2019).

76. Stålhammar-Carlemalm M, Stenberg L, Lindahl G. Protein rib: a novel group B streptococcal cell surface protein that confers protective immunity and is expressed by most strains causing invasive infections. *J Exp Med* **177**, 1593-1603 (1993).

77. Watanakunakorn C, Bakie C. Synergism of vancomycin-gentamicin and vancomycin-streptomycin against enterococci. *Antimicrob Agents Chemother* **4**, 120-124 (1973).

78. Moellering RC, Jr., Weinberg AN. Studies on antibiotic syngerism against enterococci. II. Effect of various antibiotics on the uptake of 14 C-labeled streptomycin by enterococci. *J Clin Invest* **50**, 2580-2584 (1971).

79. Pericas JM*, et al.* Changes in the treatment of *Enterococcus faecalis* infective endocarditis in Spain in the last 15 years: from ampicillin plus gentamicin to ampicillin plus ceftriaxone. *Clin Microbiol Infect* **20**, O1075-1083 (2014).

80. Gawryszewska I*, et al.* Distribution of antimicrobial resistance determinants, virulence-associated factors and clustered regularly interspaced palindromic repeats loci in isolates of *Enterococcus faecalis* from various settings and genetic lineages. *Pathog Dis* **75**, (2017).

81. Zhanel GG, Schweizer F, Karlowsky JA. Oritavancin: mechanism of action. *Clin Infect Dis* **54 Suppl 3**, S214-219 (2012).

82. Di Gregorio S, Fernandez S, Perazzi B, Bello N, Famiglietti A, Mollerach M. Increase in IS256 transposition in invasive vancomycin heteroresistant *Staphylococcus aureus* isolate belonging to ST100 and its derived VISA mutants. *Infect Genet Evol* **43**, 197-202 (2016).

83. Lee MD. GToTree: a user-friendly workflow for phylogenomics. *Bioinformatics* **35**, 4162-4164 (2019).

84. Mai U, Mirarab S. TreeShrink: fast and accurate detection of outlier long branches in collections of phylogenetic trees. *BMC Genomics* **19**, 272 (2018).

85. Letunic I, Bork P. Interactive Tree Of Life (iTOL) v4: recent updates and new developments. *Nucleic Acids Res* **47**, W256-W259 (2019).

86. Shen W, Le S, Li Y, Hu F. SeqKit: a cross-platform and ultrafast toolkit for FASTA/Q file manipulation. *PLoS One* **11**, e0163962 (2016).

87. Seemann T. mlst. *Github* - *https://githubcom/tseemann/mlst*.

88. Jolley KA, Maiden MCJ. BIGSdb: Scalable analysis of bacterial genome variation at the population level. *BMC Bioinformatics* **11**, 595 (2010).

89. Hyatt D, Chen GL, Locascio PF, Land ML, Larimer FW, Hauser LJ. Prodigal: prokaryotic gene recognition and translation initiation site identification. *BMC Bioinformatics* **11**, 119 (2010).

90. Gish W, States DJ. Identification of protein coding regions by database similarity search. *Nat Genet* **3**, 266-272 (1993).

91. Liu B, Zheng D, Jin Q, Chen L, Yang J. VFDB 2019: a comparative pathogenomic platform with an interactive web interface. *Nucleic Acids Res* **47**, D687-D692 (2018).

92. Martin M. Cutadapt removes adapter sequences from high-throughput sequencing reads. *EMBnetjournal* **17**, 3 (2011).

1003 93. Langmead B, Salzberg SL. Fast gapped-read alignment with Bowtie 2. *Nat Methods* **9**,
1004 357-359 (2012).

1005
1006 94. Li H*, et al.* The sequence alignment/map format and SAMtools. *Bioinformatics* **25**, 2078-
1007 2079 (2009).

1008
1009 95. Quinlan AR, Hall IM. BEDTools: a flexible suite of utilities for comparing genomic
1010 features. *Bioinformatics* **26**, 841-842 (2010).

1011
1012 96. Love MI, Huber W, Anders S. Moderated estimation of fold change and dispersion for
1013 RNA-seq data with DESeq2. *Genome Biol* **15**, 550 (2014).

1014
1015 97. Perez-Casal J, Caparon MG, Scott JR. Mry, a trans-acting positive regulator of the M
1016 protein gene of *Streptococcus pyogenes* with similarity to the receptor proteins of two-
1017 component regulatory systems. *J Bacteriol* **173**, 2617-2624 (1991).

1018

1019

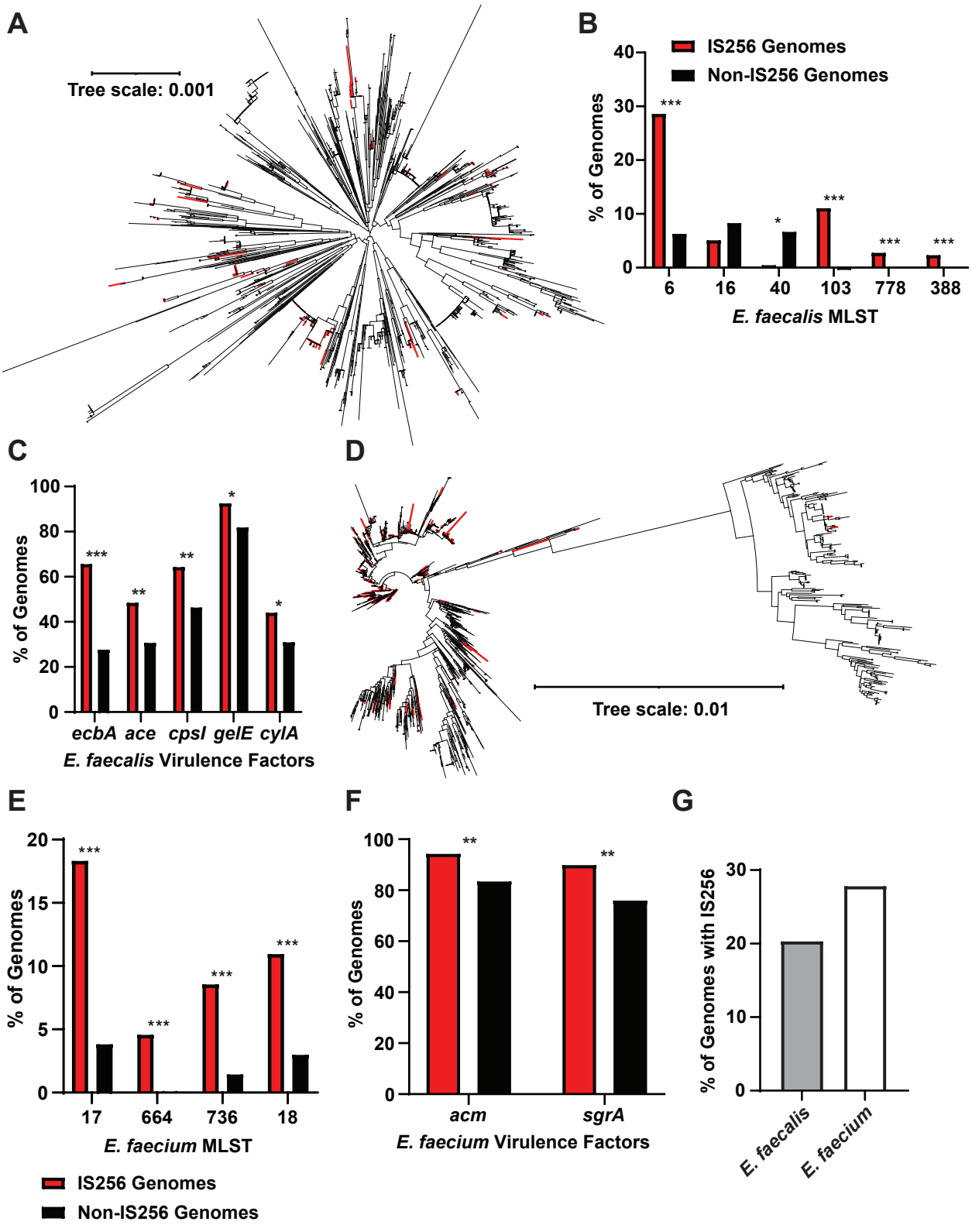


**Figure 1**

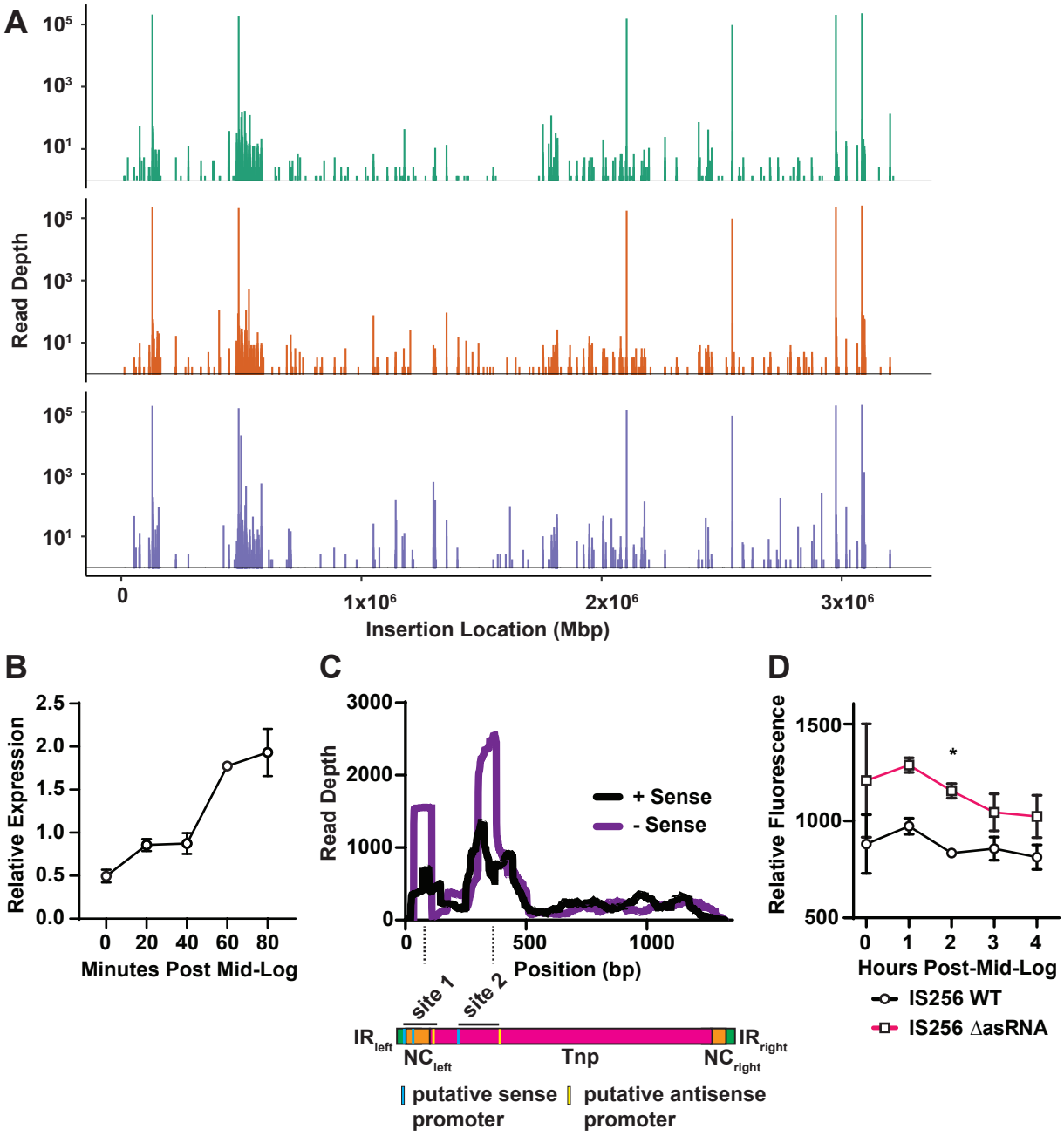


**Figure 2**

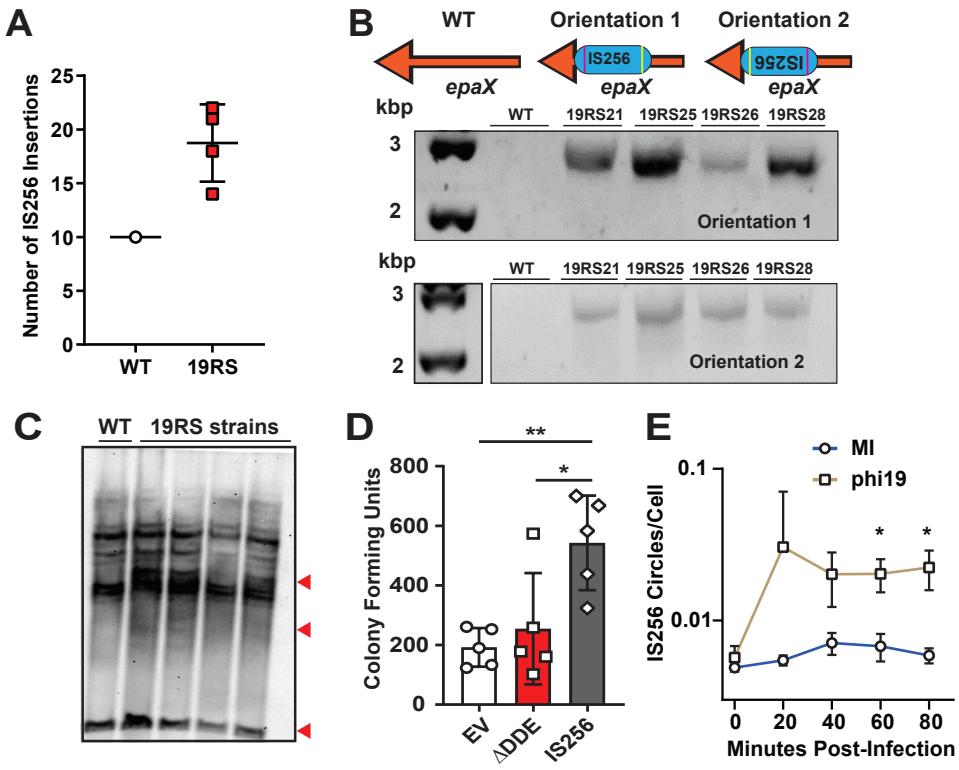


**Figure 3**

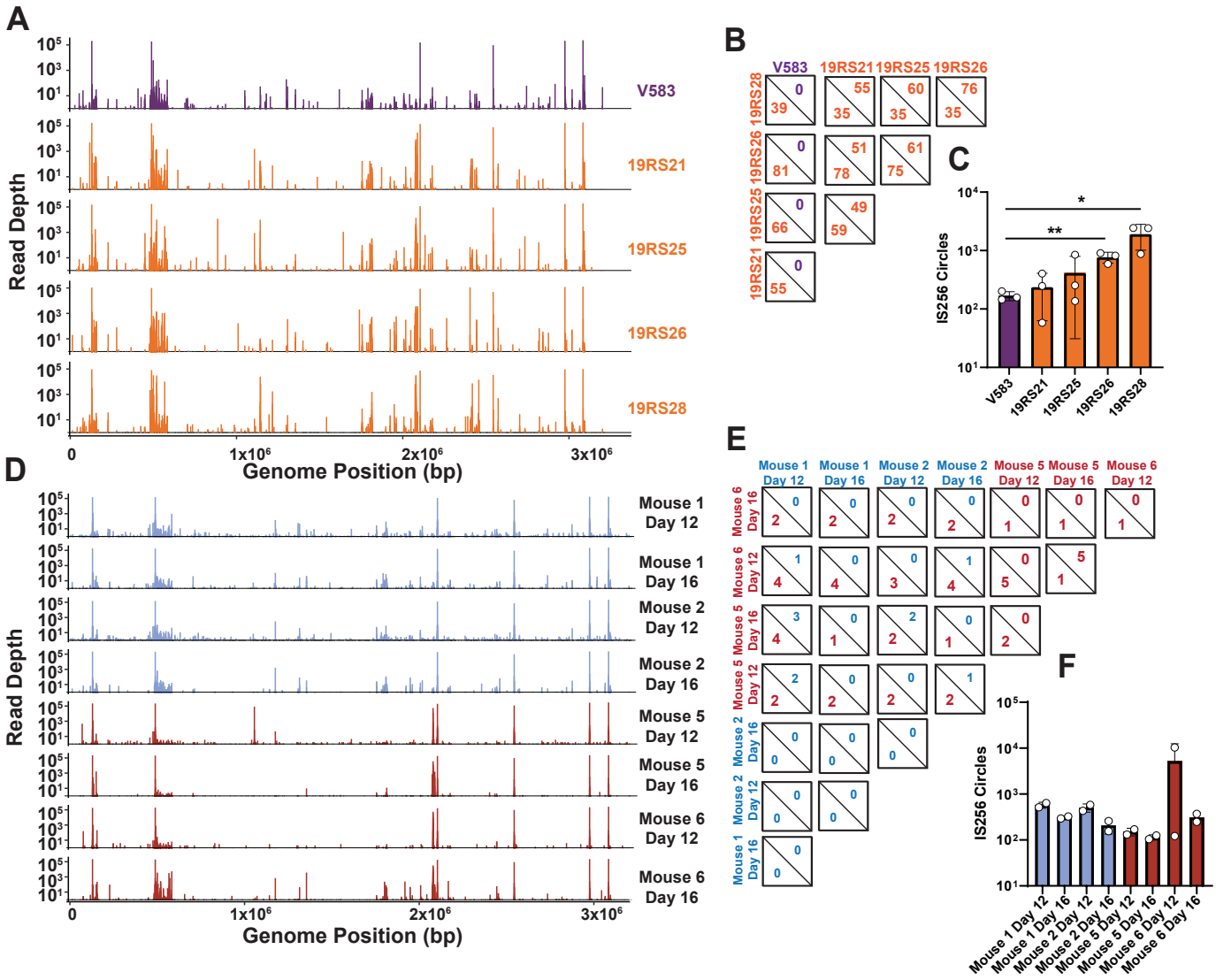


# Figure 4

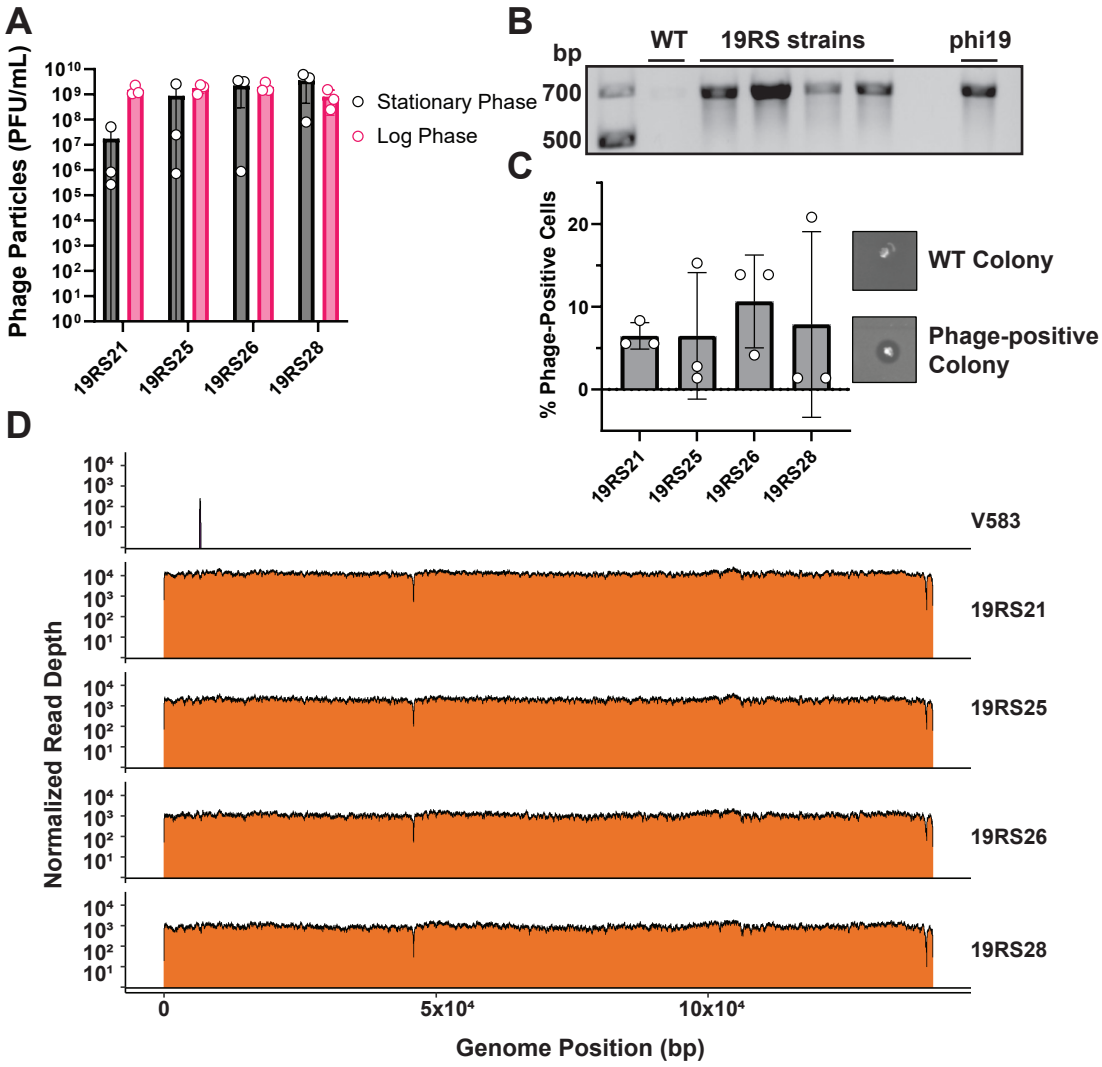


**Figure 5**

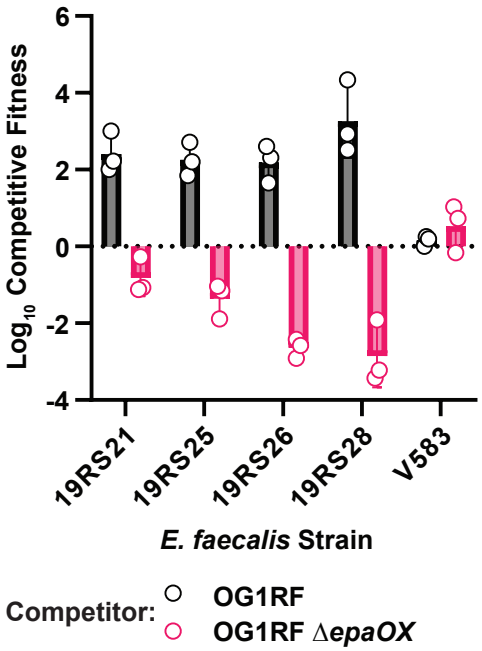


# Figure 6

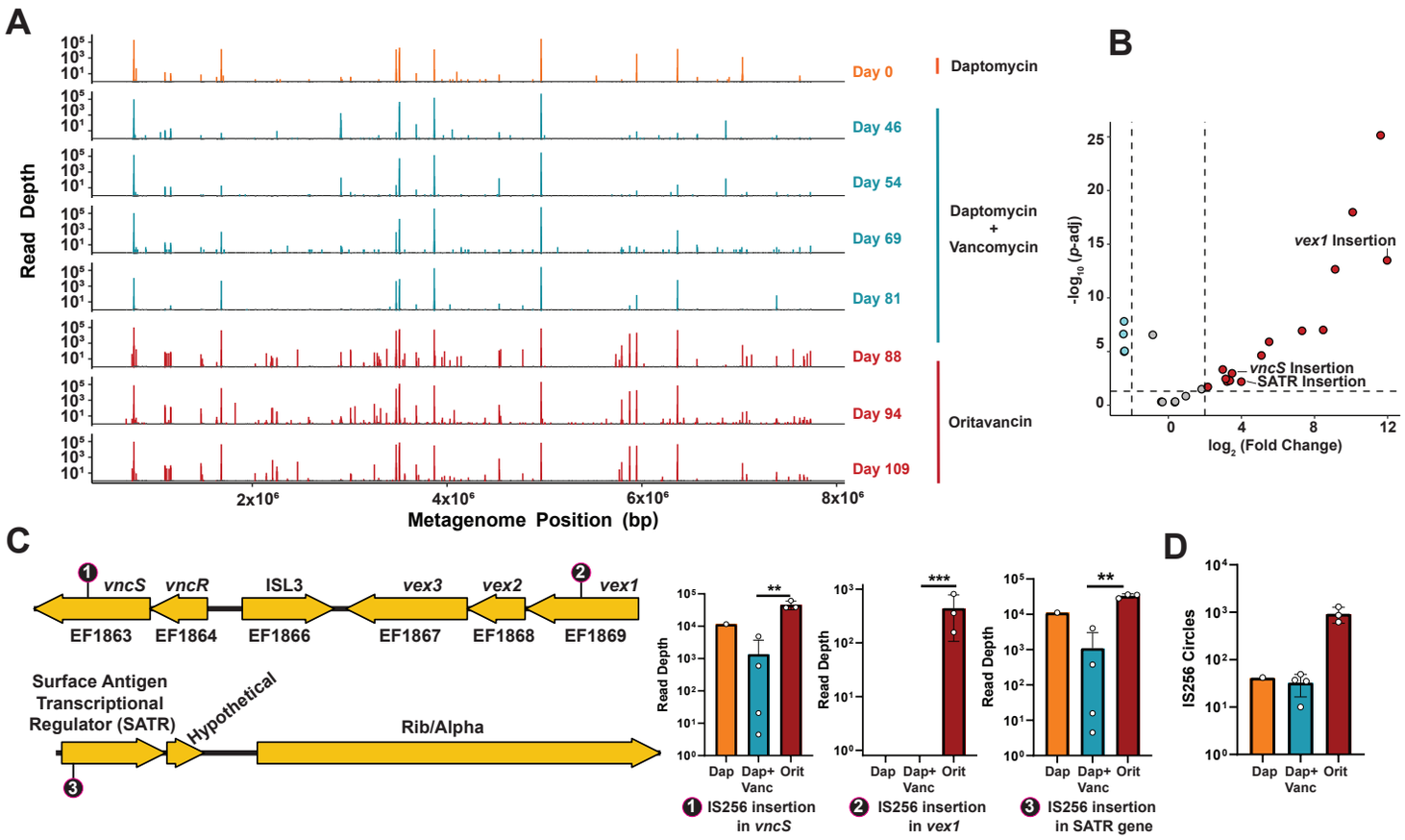


# Figure 7